

# Evolution of singularities in a partially coherent vortex beam

Thomas van Dijk<sup>1</sup> and Taco D. Visser<sup>1,2,\*</sup>

<sup>1</sup>*Department of Physics and Astronomy, Free University, De Boelelaan 1081, 1081 HV Amsterdam, The Netherlands*

<sup>2</sup>*Department of Electrical Engineering, Delft University of Technology, Mekelweg 4, 2628 CD Delft, The Netherlands*

\*Corresponding author: [tviss@nat.vu.nl](mailto:tviss@nat.vu.nl)

Received December 10, 2008; accepted January 28, 2009;  
posted February 4, 2009 (Doc. ID 104646); published March 10, 2009

We study the evolution of phase singularities and coherence singularities in a Laguerre–Gauss beam that is rendered partially coherent by letting it pass through a spatial light modulator. The original beam has an on-axis minimum of intensity—a phase singularity—that transforms into a maximum of the far-field intensity. In contrast, although the original beam has no coherence singularities, such singularities are found to develop as the beam propagates. This disappearance of one kind of singularity and the gradual appearance of another is illustrated with numerical examples. © 2009 Optical Society of America

OCIS codes: 30.1640, 050.1960, 050.4865, 260.6042.

Singular optics [1,2], the study of topological features of optical fields, has expanded in scope from phase singularities and polarization singularities [3–5] to coherence singularities. The latter kind occurs when the field at a certain frequency at one point is completely uncorrelated with the field at another point, at the same frequency [6–9]. Coherence singularities affect one of the most basic properties of a wave field, namely, its ability to produce interference patterns.

Vortex beams (sometimes called “dark core beams” or “doughnut beams”) have an on-axis zero of intensity, i.e., a phase singularity [10]. They are widely used for the guiding of atomic beams [11], for the trapping of cold atomic clouds [12], and as optical tweezers for low-index particles [13]. In addition, their relative insensitivity to atmospheric turbulence makes them candidates for optical communication [14]. The coherence properties of certain types of vortex beams have been studied by Ponomarenko and colleagues [15,16]. Theoretical and experimental studies of correlations in the time domain were reported by Swartzlander and colleagues [17–19].

It is the aim of this paper to deepen the understanding of the not yet completely clarified interplay between intensity zeros (phase singularities) and coherence singularities. We study a new type of beam, namely, a partially coherent Laguerre–Gauss beam (LG). Such a beam may be produced by letting a monochromatic, and hence fully coherent, single mode of frequency  $\omega$  pass through a phase screen [20,21], leaving its amplitude unchanged. In the case of a  $LG_1^0$  mode propagating along the  $z$  axis, the field incident on the phase screen is given by the expression ([22], Sec. 16.4)

$$U^{(\text{inc})}(\boldsymbol{\rho}, \omega) = A \exp(i\phi) \rho \exp(-\rho^2/4\sigma_S^2), \quad (1)$$

with  $A$  a constant,  $\sigma_S$  the effective source width, and  $\boldsymbol{\rho} = \rho(\cos \phi, \sin \phi)$  a two-dimensional vector that represents

a position in the plane perpendicular to the  $z$  axis. The action of the phase screen is twofold: it imprints a deterministic phase  $-\phi$  onto the beam, and in addition it randomizes the phase with a Gaussian correlation function. This can be achieved by means of a spatial light modulator (SLM). By averaging over different realizations of the SLM, a beam with the prescribed statistical behavior is obtained [23].

In the space-frequency domain, the statistical properties of a source may be characterized by its cross-spectral density function [24]

$$W^{(0)}(\boldsymbol{\rho}_1, \boldsymbol{\rho}_2, \omega) = \langle U^{(0)*}(\boldsymbol{\rho}_1, \omega) U^{(0)}(\boldsymbol{\rho}_2, \omega) \rangle, \quad (2)$$

where the asterisk denotes complex conjugation and the angular brackets indicate an ensemble average. The superscript (0) indicates positions in the secondary source plane ( $z=0$ ) immediately behind the SLM (see Fig. 1). The spectral degree of coherence is the normalized version of the cross-spectral density, viz.,

$$\mu^{(0)}(\boldsymbol{\rho}_1, \boldsymbol{\rho}_2, \omega) = \frac{W^{(0)}(\boldsymbol{\rho}_1, \boldsymbol{\rho}_2, \omega)}{\sqrt{S^{(0)}(\boldsymbol{\rho}_1, \omega) S^{(0)}(\boldsymbol{\rho}_2, \omega)}}, \quad (3)$$

with

$$S^{(0)}(\boldsymbol{\rho}, \omega) = W^{(0)}(\boldsymbol{\rho}, \boldsymbol{\rho}, \omega) = A^2 \rho^2 \exp(-\rho^2/2\sigma_S^2), \quad (4)$$

the spectral density (or “intensity at frequency  $\omega$ ”). The spectral degree of coherence caused by the SLM is homogeneous and Gaussian, i.e.,

$$\mu^{(0)}(\boldsymbol{\rho}_1, \boldsymbol{\rho}_2, \omega) = \mu^{(0)}(\boldsymbol{\rho}_2 - \boldsymbol{\rho}_1, \omega) = \exp[-(\rho_2 - \rho_1)^2/2\sigma_\mu^2], \quad (5)$$

with  $\sigma_\mu$  the effective coherence length of the secondary source. On substituting from Eqs. (4) and (5) into Eq. (3) we find that the cross-spectral density takes the form

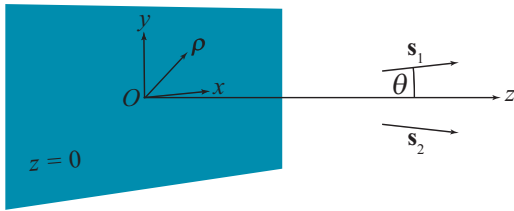


Fig. 1. (Color online) Illustration of the notation.

$$W^{(0)}(\boldsymbol{\rho}_1, \boldsymbol{\rho}_2, \omega) = A^2 \rho_1 \rho_2 \exp[-(\rho_1^2 + \rho_2^2)/4\sigma_S^2] \times \exp[-(\rho_2 - \rho_1)^2/2\sigma_\mu^2]. \quad (6)$$

We notice that Eq. (4) indicates the presence of an on-axis phase singularity in the source plane, i.e.,  $S^{(0)}(\boldsymbol{\rho}=0, \omega) = 0$ . Coherence singularities occur when the phase of the spectral degree of coherence is undefined, i.e., when  $\mu^{(0)} \times (\boldsymbol{\rho}_1, \boldsymbol{\rho}_2, \omega) = 0$ . In that case, the combination of the fields at  $\boldsymbol{\rho}_1$  and  $\boldsymbol{\rho}_2$  in a Young's type experiment yields an interference pattern without spatial modulation. Equation (5) implies that no such singularities exist in the source plane.

A source is said to be quasi-homogeneous if its spectral degree of coherence  $\mu^{(0)}(\boldsymbol{\rho}', \omega)$  varies much more rapidly with  $\boldsymbol{\rho}'$  than its spectral density  $S^{(0)}(\boldsymbol{\rho}, \omega)$  varies with  $\boldsymbol{\rho}$ . In that case the radiant intensity (defined as  $r^2$  times the far-field spectral density) and the spectral degree of coherence of the field in the far zone are related to the same properties in the source plane by the reciprocity relations ([24], Sec. 5.3.2)

$$J(\mathbf{s}, \omega) = (2\pi k)^2 \tilde{S}^{(0)}(0, \omega) \tilde{\mu}^{(0)}(k\mathbf{s}_\perp, \omega) \cos^2 \theta, \quad (7)$$

$$\mu^{(\infty)}(r_1 \mathbf{s}_1, r_2 \mathbf{s}_2, \omega) = \tilde{S}^{(0)}[k(\mathbf{s}_{2\perp} - \mathbf{s}_{1\perp}), \omega] \times \exp[ik(r_2 - r_1)] / \tilde{S}^{(0)}(0, \omega), \quad (8)$$

with the two-dimensional Fourier transforms given by the expressions

$$\tilde{S}^{(0)}(\mathbf{f}, \omega) = \frac{1}{(2\pi)^2} \int S^{(0)}(\boldsymbol{\rho}, \omega) e^{-i\mathbf{f} \cdot \boldsymbol{\rho}} d^2 \boldsymbol{\rho}, \quad (9)$$

$$\tilde{\mu}^{(0)}(\mathbf{f}, \omega) = \frac{1}{(2\pi)^2} \int \mu^{(0)}(\boldsymbol{\rho}, \omega) e^{-i\mathbf{f} \cdot \boldsymbol{\rho}} d^2 \boldsymbol{\rho}. \quad (10)$$

Here  $k = 2\pi/\lambda$  is the wavenumber associated frequency  $\omega$ ,  $\mathbf{s}_\perp$  is the projection of the unit direction vector  $\mathbf{s}$  onto the  $xy$  plane, and  $\theta$  is the angle that the  $\mathbf{s}$  direction makes with the  $z$  axis (see Fig. 1). The superscript  $(\infty)$  indicates points in the far zone. On substituting from Eqs. (4) and (5) into Eqs. (9) and (10) while using the theorem for Fourier transforms of derivatives, we find that

$$\tilde{S}^{(0)}(\mathbf{f}, \omega) = (2 - f^2 \sigma_S^2) \sigma_S^4 A^2 \exp(-f^2 \sigma_S^2/2)/2\pi, \quad (11)$$

$$\tilde{\mu}^{(0)}(\mathbf{f}, \omega) = \sigma_\mu^2 \exp(-f^2 \sigma_\mu^2/2)/2\pi. \quad (12)$$

On choosing the two observation points to be symmetrically positioned with respect to the  $z$  axis, i.e.,  $r_1 = r_2 = r$  and  $\mathbf{s}_{2\perp} = -\mathbf{s}_{1\perp} = (\sin \theta, 0)$ , we obtain the formulas

$$J(\mathbf{s}, \omega) = 2k^2 \sigma_S^4 \sigma_\mu^2 A^2 \cos^2 \theta \exp(-k^2 \sigma_\mu^2 \sin^2 \theta/2), \quad (13)$$

$$\mu^{(\infty)}(r\mathbf{s}_1, r\mathbf{s}_2, \omega) = [1 - 2k^2 \sigma_S^2 \sin^2 \theta] \exp(-2k^2 \sigma_S^2 \sin^2 \theta). \quad (14)$$

These last two results indicate that the character of the field singularities changes as the beam propagates: Eq. (13) shows that the on-axis intensity, a phase singularity in the source plane, transforms into a maximum of the far-zone radiant intensity; and Eq. (14) implies that, in contrast to the source plane, there are pairs of points in the far zone at which the field is completely uncorrelated. Coherence singularities, i.e.,  $\mu^{(\infty)}(r\mathbf{s}_1, r\mathbf{s}_2, \omega) = 0$ , occur at observation points for which the term between square brackets in Eq. (14) vanishes. This happens for observation angles  $\theta_{CS}$  such that

$$\sin \theta_{CS} = (2k^2 \sigma_S^2)^{-1/2}. \quad (15)$$

It is to be noted that this behavior is quite different from that of the class of partially coherent vortex beams described earlier [15,16]. Those beams, being an incoherent superposition of Laguerre–Gauss modes, retain their on-axis phase singularity on propagation. We mention in passing that Eq. (13) implies that in order for the field to be beamlike, the source has to satisfy the condition

$$k^2 \sigma_\mu^2/2 \gg 1. \quad (16)$$

The reciprocity relations (7) and (8) describe the connection between the field in the source plane and that in the far zone. However, they do not describe how the initial on-axis phase singularity changes on propagation or how the coherence singularity comes into existence. In order to investigate this, we study the propagation of the cross-spectral density function to an arbitrary transverse plane. We have ([24], Sec. 5.6.3)

$$W(\boldsymbol{\rho}_1, \boldsymbol{\rho}_2, z, \omega) = \iint_{(z=0)} W^{(0)}(\boldsymbol{\rho}'_1, \boldsymbol{\rho}'_2, \omega) G^{\infty}(\boldsymbol{\rho}_1, \boldsymbol{\rho}'_1, z, \omega) \times G(\boldsymbol{\rho}_2, \boldsymbol{\rho}'_2, z, \omega) d^2 \rho'_1 d^2 \rho'_2, \quad (17)$$

with the paraxial Green's function given by the expression

$$G(\boldsymbol{\rho}, \boldsymbol{\rho}', z, \omega) = -\frac{ik}{2\pi z} \exp(ikz) \exp[ik(\boldsymbol{\rho} - \boldsymbol{\rho}')^2/2z]. \quad (18)$$

On substituting from Eqs. (6) into Eq. (17) we obtain after some calculations for the on-axis spectral density the formula

$$S(\boldsymbol{\rho} = 0, z, \omega) = W(\boldsymbol{\rho}_1 = 0, \boldsymbol{\rho}_2 = 0, z, \omega) \quad (19)$$

$$= \left(\frac{kA}{z}\right)^2 \int_0^\infty \int_0^\infty \rho_1'^2 \rho_2'^2 \exp(-\rho_1'^2/2\sigma_+^2) \exp(-\rho_2'^2/2\sigma_-^2) \times I_0(\rho_1' \rho_2' / \sigma_\mu^2) d\rho_1' d\rho_2', \quad (20)$$

with  $I_0(x)$  the modified Bessel function of the first kind of order zero, and

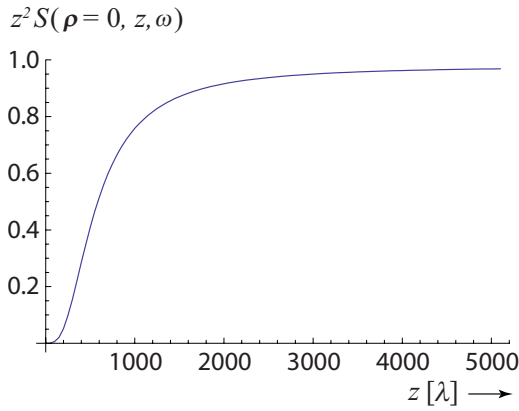


Fig. 2. (Color online) Scaled on-axis spectral density  $z^2 S(\rho=0, z, \omega)$ , calculated from Eq. (20), normalized by the radiant intensity in the forward direction  $J[\mathbf{s}=(0,0,1), \omega]$ . In this example  $\sigma_S=15\lambda$  and  $\sigma_\mu=4\lambda$ .

$$\frac{1}{2\sigma_\pm^2} = \frac{1}{4\sigma_S^2} + \frac{1}{2\sigma_\mu^2} \pm \frac{ik}{2z}. \quad (21)$$

Equation (20) can be integrated numerically for  $z \gg \lambda$ . An illustration of the behavior of the scaled on-axis spectral density  $z^2 S(\rho=0, z, \omega)$  is shown in Fig. 2, with the limiting value given by Eq. (4) added. It is seen that on propagation the phase singularity immediately evolves into a finite-valued intensity that gradually rises toward its asymptotic value, namely, that of the radiant intensity in the forward direction  $J[\mathbf{s}=(0,0,1), \omega]$ , as given by Eq. (13).

In Fig. 3 the spectral density  $S(\rho, z, \omega)$  is shown for several cross sections of the beam. As can be seen, the on-axis spectral density (initially a phase singularity) gradually rises and changes from being a minimum in the source plane to being a maximum in the far field.

The evolution of the coherence singularity is depicted in Fig. 4. There the behavior of  $|\mu(\rho, z, -\rho, z, \omega)|$  is shown shown for pairs of points on the lines of observation  $\arctan(\rho/z) = \theta_{CS}$ , the angle defined by Eq. (15), i.e., the two lines on which a correlation singularity occurs in the far zone. The modulus of the spectral degree of coherence gradually decreases as the beam propagates and eventually becomes zero, meaning that the two points form a coherence singularity.

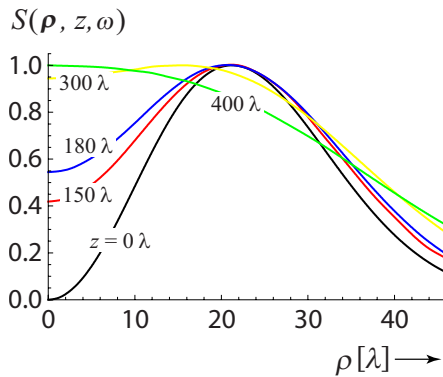


Fig. 3. (Color online) Normalized spectral density  $S(\rho, z, \omega)$ , calculated from Eq. (17), in several cross sections of the beam. In this example  $\sigma_S=15\lambda$  and  $\sigma_\mu=4\lambda$ .

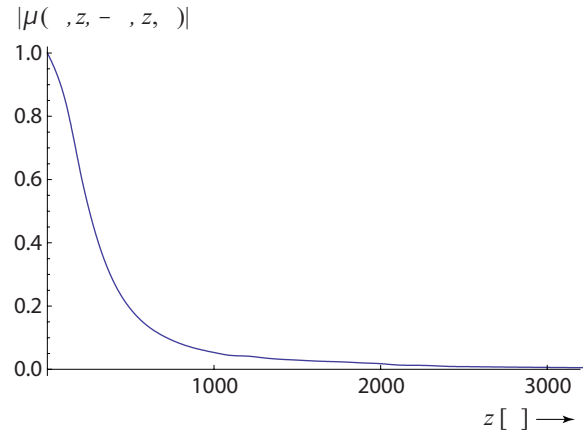


Fig. 4. (Color online) Evolution of the modulus of the spectral degree of coherence, as calculated from Eq. (17), along the two directions of observation at which a coherence singularity occurs in the far field. In this example  $\sigma_S=15\lambda$  and  $\sigma_\mu=4\lambda$ .

The behavior of the far-zone state of coherence is further analyzed by considering the spectral degree of coherence of two observation points that lie on a circle centered around the  $z$  axis [see Fig. 5(a)]. One point is kept fixed, whereas the other point is moved around the circle; i.e., we choose

$$\mathbf{s}_{1\perp} = (\sin \theta, 0), \quad (22)$$

$$\mathbf{s}_{2\perp} = (\sin \theta \cos \phi, \sin \theta \sin \phi), \quad (23)$$

and study the dependence of the spectral degree of coherence as a function of the angle  $\phi$ . We now obtain from Eq. (8) the expression

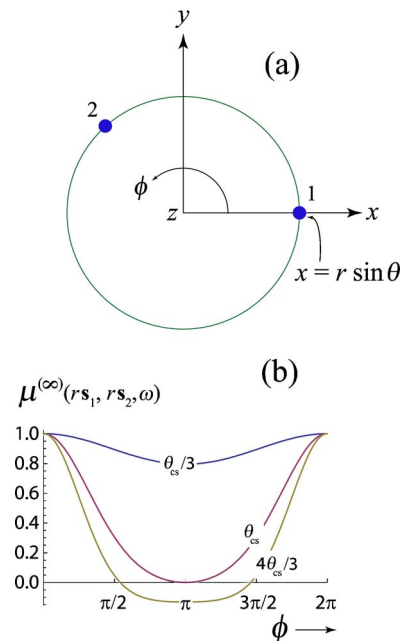


Fig. 5. (Color online) (a) Position of two far-zone observation points (dots) on a circle centered around the  $z$  axis. (b) The spectral degree of coherence of the field at the two points as a function of the angle  $\phi$  for three values of  $\theta$ . In this example  $\sigma_S=15\lambda$  and  $\sigma_\mu=4\lambda$ .

$$\mu^{(\infty)}(r\mathbf{s}_1, r\mathbf{s}_2, \omega) = [1 - 2k^2\sigma_S^2 \sin^2 \theta \sin^2(\phi/2)] \\ \times \exp[-2k^2\sigma_S^2 \sin^2 \theta \sin^2(\phi/2)]. \quad (24)$$

Equation (24) shows that the spectral degree of coherence in this case is real valued. For small circles, for which the angle  $\theta < \theta_{CS}$ ,  $\mu^{(\infty)}(r\mathbf{s}_1, r\mathbf{s}_2, \omega)$  is always positive and no coherence singularities occur [see Fig. 5(b)]. If  $\theta = \theta_{CS}$ , there is precisely one zero of the spectral degree of coherence, and the two points that lie diagonally opposite each other on the circle ( $\phi = \pi$ ) form a correlation singularity. When  $\theta$  is further increased, two zeros occur; i.e., the singularity unfolds into a doublet.

In summary, we have analyzed the behavior of a partially coherent Laguerre–Gauss beam and found a new kind of behavior of its singularities. The initial on-axis phase singularity evolves into a maximum of the radiant intensity. In contrast, a coherence singularity gradually develops as the beam propagates. As the angle between two far-field observation points is increased, this singularity unfolds into a doublet.

## ACKNOWLEDGMENTS

This research is supported by The Netherlands Organisation for Scientific Research (NWO), by the Foundation for Fundamental Research on Matter (FOM), and by the Dutch Technology Foundation (STW).

## REFERENCES

- J. F. Nye, *Natural Focusing and Fine Structure of Light* (IOP, 1999).
- M. S. Soskin and M. V. Vasnetsov, in *Progress in Optics, Vol. 42*, E. Wolf, ed. (Elsevier, Amsterdam, 2001), pp. 219–275.
- M. V. Berry and M. R. Dennis, “Polarization singularities in isotropic random vector waves,” *Proc. R. Soc. London, Ser. A* **457**, 141–155 (2001).
- I. Freund, A. I. Mokhun, M. S. Soskin, O. V. Angelsky, and I. I. Mokhun, “Stokes singularity relations,” *Opt. Lett.* **27**, 545–547 (2002).
- R. W. Schoonover and T. D. Visser, “Polarization singularities of focused, radially polarized fields,” *Opt. Express* **14**, 5733–5745 (2006).
- H. F. Schouten, G. Gbur, T. D. Visser, and E. Wolf, “Phase singularities of the coherence functions in Young’s interference pattern,” *Opt. Lett.* **28**, 968–970 (2003).
- D. G. Fischer and T. D. Visser, “Spatial correlation properties of focused partially coherent light,” *J. Opt. Soc. Am. A* **21**, 2097–2102 (2004).
- G. Gbur and T. D. Visser, “Phase singularities and coherence vortices in linear optical systems,” *Opt. Commun.* **259**, 428–435 (2006).
- T. D. Visser and R. W. Schoonover, “A cascade of singular field patterns in Young’s interference experiment,” *Opt. Commun.* **281**, 1–6 (2008).
- J. Yin, W. Gao, and Y. Zhu, “Generation of dark hollow beams and their applications,” in *Progress in Optics, Vol. 45*, E. Wolf, ed. (North Holland, 2003), pp. 119–203.
- Z. Wang, M. Dai, and J. Yin, “Atomic (or molecular) guiding using a blue-detuned doughnut mode in a hollow metallic waveguide,” *Opt. Express* **13**, 8406–8423 (2005).
- T. Kuga, Y. Torii, N. Shiokawa, T. Hirano, Y. Shimizu, and H. Sasada, “Novel optical trap of atoms with a doughnut beam,” *Phys. Rev. Lett.* **78**, 4713–4716 (1997).
- K. T. Gahagan and G. A. Swartzlander, Jr., “Simultaneous trapping of low-index and high-index microparticles observed with an optical-vortex trap,” *J. Opt. Soc. Am. B* **16**, 533–537 (1999).
- G. Gbur and R. K. Tyson, “Vortex beam propagation through atmospheric turbulence and topological charge conservation,” *J. Opt. Soc. Am. A* **25**, 225–230 (2008).
- S. A. Ponomarenko, “A class of partially coherent beams carrying optical vortices,” *J. Opt. Soc. Am. A* **18**, 150–156 (2001).
- G. V. Bogatyryova, C. V. Fel’de, P. V. Polyanskii, S. A. Ponomarenko, M. S. Soskin, and E. Wolf, “Partially coherent vortex beams with a separable phase,” *Opt. Lett.* **28**, 878–880 (2003).
- D. M. Palacios, I. D. Maleev, A. S. Marathay, and G. A. Swartzlander, Jr., “Spatial correlation singularity of a vortex field,” *Phys. Rev. Lett.* **92**, 143905 (2004).
- G. A. Swartzlander, Jr., and J. Schmit, “Temporal correlation vortices and topological dispersion,” *Phys. Rev. Lett.* **93**, 093901 (2004).
- I. D. Maleev and G. A. Swartzlander, Jr., “Propagation of spatial correlation vortices,” *J. Opt. Soc. Am. B* **25**, 915–922 (2008).
- L. C. Andrews and R. L. Phillips, *Laser Beam Propagation through Random Media*, 2nd ed. (SPIE Press, 2005).
- J. W. Goodman, *Statistical Optics* (Wiley, New York, 2000). See Chap. 8.3.
- A. E. Siegman, *Lasers* (University Science Books, 1986).
- D. C. Dayton, S. L. Browne, S. P. Sandven, J. D. Goglewski, and A. V. Kudryashov, “Theory and laboratory demonstrations on the use of a nematic liquid-crystal phase modulator for controlled turbulence generation and adaptive optics,” *Appl. Opt.* **37**, 5579–5589 (1998).
- L. Mandel and E. Wolf, *Optical Coherence and Quantum Optics* (Cambridge, 1995).